Journal of Applied Science and Engineering Innovation, Vol.10, No.1, 2023, pp. 21-30
ISSN (Print): 2331-9062
ISSN (Online): 2331-9070

Short-Term Load Forecasting Method Based on LSTM-SVR Considering Generalized Demand-Side Resources

Peixin Chang, Xin Zhao, Yu Niu, Huanhuan Zhang
Lanzhou University of Technology, 730050, Lanzhou, Gansu, China
3057342712@qq.com

Abstract: With the continuous development of smart grid, a large number of generalized demand-side resources such as controllable load, energy storage and distributed power generation are accessed, which changes the characteristics of load and increases the difficulty of load forecasting. In order to improve the accuracy of load forecasting, this paper proposes a short-term load forecasting method of LSTM-SVR considering generalized demand-side resources. Firstly, according to the load aggregator, the mechanism of generalized demand-side resources participating in the power market is determined, a contract-based generalized demand-side resource scheduling model is constructed, and the optimal dispatching plan is solved according to this model. Secondly, the LSTM-SVR combined forecasting method is used to establish a short-term load forecasting model with the optimal scheduling plan as the input. Finally, a case analysis is carried out, and the feasibility of the LSTM-SVR prediction method considering generalized demand-side resources is verified by comparison with other models.
Keywords Short-term load forecasting; Broad demand-side resources; LSTM-SVR; Error correction; Load aggregator

INTRODUCTION

Short-term load forecasting is of great significance for economic dispatch, optimal combination of units, optimal power flow, and power market trading. Its biggest feature is that it has obvious periodicity, which is mainly manifested in the similarity of the overall change law of 24 hours between different days, the similarity of working days or rest days, and the similarity of the load curves of major holidays in different years. Accurate load forecasting is conducive to improving the utilization rate of power generation equipment and the economy of dispatching, and maintaining the safety and stability of power grid operation [Jia Hongjie, *et al*., 2015]. Generalized demand-side resources such as controllable load, distributed power and energy storage in the smart grid respond to demand in flexible and diverse ways, which enhances load transfer capacity and a wider transferable time range [Wu Jianzhong, *et al*., 2016].

In the power market environment, users take electricity economy as the goal, reasonably adjust controllable load, distributed power source and energy storage resources according to different price signals and incentive mechanisms, and change load characteristics and change laws [Rastegar M, *et al*., 2016]. Therefore, short-term load forecasting considers generalized demand-side resources to improve load forecasting accuracy.

The ideas of short-term load forecasting include normal daily forecasting based on time series analysis, short-term load forecasting that directly considers related factors, short-term load forecasting after normalization of related factors, and probabilistic short-term load forecasting. With the continuous development of computer technology, the algorithms of short-term load forecasting have been optimized from early regression analysis methods and time series methods to intelligent algorithms such as artificial neural networks and ensemble learning, which greatly improves the efficiency and accuracy of short-term load forecasting. For example, support vector machines, long short-term memory neural networks, and random forests have obvious advantages in processing nonlinear data. There is always a random factor in the load, so there is no way to avoid errors in the prediction results of the model. By analyzing the residual between the predicted and true values of the model, modeling the residual series to correct the load forecast is an effective means. It has proven its effectiveness in a variety of predictions such as temperature, wind speed, wind power and photovoltaic power [Kang Chongqing, *et al*., 2017].

Generalized demand-side resources such as controllable load, distributed power and energy storage are widely connected and participate in the power market, and their scheduling flexibility will inevitably affect the change of electricity load. Therefore, this paper first constructs a contract-based optimal scheduling model for generalized demand-side resources for three controllable resources: load curtailment (LC)， load shift (LS) and interruptible load (IL). The model aims to maximize the return of load aggregator (LA), and solves the optimal dispatching strategy of generalized demand-side resources participating in the power market according to the real-time electricity price under the constraints of the contract. Based on this, the LSTM-SVR load forecasting model is introduced, and the optimal

Corresponding Author: Peixin Chang, College of Electrical and Information Engineering, Lanzhou University of Technology, Lanzhou, 730050, Gansu, China.

scheduling plan of generalized demand-side resources

load forecasting method based on the optimal scheduling plan of generalized demand-side resources is proposed, and an example is verified.

The main contributions of this paper are summarized as follows.

(I) This paper takes the benefits of aggregators as the biggest goal, and solves the optimal dispatching strategy for generalized demand-side resources to participate in the power market based on real-time electricity prices.

(II) Compared with the traditional load forecasting method, this paper considers the generalized demand-side resources as the input of the forecasting model, which effectively reduces the peak-valley difference of the load.

(III) Based on the LSTM prediction model, SVR is used to correct the error and improve the prediction accuracy.

Section II proposes a contract-based generalized demand-side scheduling model, including a transferable load contract model and a reducible load contract model. Section III proposes a load forecasting model based on LSTM-SVR, uses SVR to correct the error of LSTM, and gives the input amount of the prediction model. Section IV. is the analysis of the actual example, first solving the scheduling model, and then carrying out load forecasting, which shows the superiority of this method through a variety of comparisons. Finally, the full text is summarized in Part V.

GENERALIZED DEMAND-SIDE SCHEDULING MODEL BASED ON CONTRACT

LA acts as an intermediary that can integrate user demand response resources and introduce them into market transactions. With the help and guidance of LA, small and medium-sized power users can form a scientific way of electricity consumption and improve the power efficiency of terminal equipment. The operation mechanism of LA is shown in Figure 1.

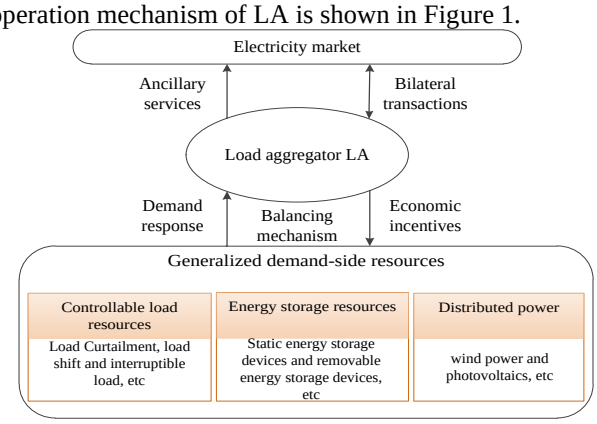

Figure 1. The operating mechanism of LA

In order to guide users to better participate in market regulation, this section proposes a contract-based generalized demand-side resource scheduling model from the perspective of LA. LA can enter into different contracts with users based on factors such as electricity prices and electricity consumption characteristics in the area where the aggregated electricity users are located. Among them, the differences in contracts are mainly reflected in the design of agreed price, response volume and response period. According to the difference between the real-time electricity price in the electricity market and the price agreed in the contract, the goal is to maximize the income, and the optimal dispatch plan of LC, LS and IL is determined under the provisions of the contract content, and the user is guided to reasonably arrange the power consumption time to achieve the role of peak shaving and valley filling.

Load curtailment contract model

Load curtailment generally refers to a load that can be reduced to some extent as needed. LA enters into executable LC contracts with small and medium-sized households, and arranges the optimal period for load reduction according to the difference between the contracted price and the real-time electricity price in the electricity market, so as to obtain maximum profit and achieve peak shaving efficiency. The objective function of the LC contract model is:

$$\max \sum_{t\in T}\left(\rho_t L_t^{LC} - C_t^{LC}\right) \tag{1}$$

Where, ρ_t is the real-time electricity price in the electricity market, L_t^{LC} is the total load reduction of LC at time t, C_t^{LC} is the total cost of the LC contract at time t, and T is the number of time series in a day. The function for L_t^{LC} and C_t^{LC} is as follows:

$$L_t^{LC} = \sum_{k\in N_{LC}} q_k^{LC} u_{kt}^{LC} \tag{2}$$

$$C_t^{LC} = \sum_{k\in N_{LC}} \left(\mathrm{IC}_k^{LC} y_{kt}^{LC} + c_k^{LC} q_k^{LC} u_{kt}^{LC}\right) \tag{3}$$

Where, q_k^{LC}、IC_k^{LC} and c_k^{LC} are the load reduction amount, start-up cost and price specified in the k-th LC contract, and u_{kt}^{LC} is the load reduction status index. When the k-th LC contract is executed at time t, $u_{kt}^{LC}=1$ otherwise, $u_{kt}^{LC}=0$. y_{kt}^{LC} is the LC contract start-up index, When the k-th LC contract is activated at time t, $y_{kt}^{LC}=1$, otherwise, $y_{kt}^{LC}=0$. N_{LC} is the contract quantity. The contract is subject to:

$$\sum_{t'=t}^{t+D_k^{\min,LC}-1} \mathrm{u}_{kt'}^{LC} \geq D_k^{\min,LC} y_{kt}^{LC} \qquad \forall k,t, \tag{4}$$

$$\sum_{t'=t}^{t+D_k^{\max,LC}-1} z_{kt'}^{LC} \geq y_{kt}^{LC} \qquad \forall k,t, \tag{5}$$

$$\sum_{t\in T} y_{kt}^{LC} \le MN_k^{LC} \quad \forall k,t, \tag{6}$$

$$y_{kt}^{LC} - z_{kt}^{LC} = u_{kt}^{LC} - u_{k(t-1)}^{LC} \quad \forall k,t, \tag{7}$$

$$y_{kt}^{LC} + z_{kt}^{LC} \le 1 \quad \forall k,t, \tag{8}$$

Where, $D_k^{\min,LC}$ and $D_k^{\max,LC}$ are the minimum and maximum duration of the contract, respectively. MN_k^{LC} is the maximum number of contract executions per day, z_{kt}^{LC} is the contract stop indicator. When the kth LC contract stops at time t, $z_{kt}^{LC}=1$, otherwise, $z_{kt}^{LC}=0$. It can be seen that constraints (4) - (6) are the limits of the minimum duration, maximum duration and maximum number of daily contract executions, respectively, and constraint (7) controls the contract start-stop index. Constraint (8) ensures that y_{kt}^{LC} and z_{kt}^{LC} are not 1s at the same time.

Load shift contract model

Load shift usually refers to the constant total electricity consumption during a dispatch cycle. Loads that can be flexibly adjusted for electricity consumption at different times. LA acts as a shift to fill valleys by guiding customers to shift electricity consumption from the contracted period of load reduction to the period of load increase. It can be expressed as:

$$\max \sum_{t\in T} \left(\rho_t \mathrm{L}_t^{LS} - C_t^{LS}\right) \tag{9}$$

$$L_t^{LS} = \sum_{k\in N_{LS}} q_k^{LS} u_{kt}^{LS} \tag{10}$$

$$C_t^{LS} = \sum_{k\in N_{LS}} \left(IC_k^{LS} y_{kt}^{LS} + c_k^{LS} q_k^{LS} u_{kt}^{LS}\right) \tag{11}$$

$$\sum_{t\in \mathrm{T}} q_{kt}^{LS} \alpha_{kt}^{LS} = 0, \forall k \tag{12}$$

Equation (12) is the constraint of change before and after transferable load scheduling, where α_{kt}^{LS} represents the transfer direction of the load at time t, $\alpha_{kt}^{LS}=-1$ indicates that the load is transferred out at this time, $\alpha_{kt}^{LS}=0$ indicates that there is no transfer load at this time, and $\alpha_{kt}^{LS}=1$ indicates that the load is transferred in at this time. The contract is subject to:

$$\sum_{t'=t}^{t+\mathrm{D}_k^{\min,LS}-1} u_{kt'}^{LS} \ge D_k^{\min,LS} y_{kt}^{LS}, \forall k,t \tag{13}$$

$$\sum_{t'=t}^{t+D_k^{\max,LS}-1} z_{kt'}^{LS} \ge y_{kt}^{LS} \quad \forall k,t, \tag{14}$$

$$\sum_{t\in T} y_{kt}^{LS} \le MN_k^{LS} \quad \forall k, \tag{15}$$

$$y_{kt}^{LS} - z_{kt}^{LS} = u_{kt}^{LS} - u_{k(t-1)}^{LS} \quad \forall k,t, \tag{16}$$

$$y_{kt}^{LS} + z_{kt}^{LS} \le 1 \quad \forall k,t, \tag{17}$$

$$u_{kt}^{LS} = 0 \ \forall t \notin T_k^{LS}, \tag{18}$$

Where, T_k^{LS} is the load transfer time period, constraint (18) restricts the execution of the LS contract during T_k^{LS}, and variables and constraints such as L_t^{LS}, C_t^{LS}, q_k^{LS}, IC_k^{LS} and c_k^{LS} are similar to the LC model.

Interruptible load contract model

The load aggregator revenue for interruptible loads is the sum of the interruption compensation received from the grid, additional subsidies and project management fees paid by users. The cumulative maximum return of the l-th aggregator as an objective function:

$$\max \sum_{m=1}^{T} (a \times \Delta Q_{LAlm} + B_{eLAlm} + \sum_{i\in\varphi_l} C_{xulim}) \tag{19}$$

$$l = 1,2,\cdots,N$$

Where, a is the interruption compensation price of the power grid to the aggregator; ΔQ_{LAlm}, B_{eLAlm} are the power outage in the m-th year of the l-th aggregator and the upfront subsidy paid to the user, $\Delta Q_{LAlm} = \sum_{i\in\varphi_l} t_{lim} \times P_{uli}$, $B_{eLAlm} = \sum_{i\in\varphi_l} B_{eim}$; C_{xulim}

The project management fee paid for the m-th year of the i-th user managed by the lth aggregator is usually higher than C_{LAlim}.

Considering that the load aggregator, as an intermediary, should ensure that the maximum interruptible resources are called, it is proposed that according to the signing of the contract with the user, the following constraints need to be met when signing the contract with the power grid, that is, the interrupt capacity is less than or equal to the total capacity of the user that can be interrupted, the total electricity consumption is less than or equal to the total power consumption of the user, and the total interruption time is less than or equal to the total interruption time of the user's participation in the user:

$$L_t^{IL,d} \le \sum_{i=1}^{n} P_{ui} \tag{20}$$

$$L_t^{IL,d} \times k_{LA} \times t_{LA} \le \sum_{i=1}^{n} P_{ui} \times t_{ui} \tag{21}$$

$$t_{LA} \times k_{LA} \le \sum_{i=1}^{n} t_{ui} \tag{22}$$

Where, , k_{LA}, and t_{LA} are the interrupt capacity, the number of interruptions, and the number of hours of interruption in the contract signed between the load

aggregator and the power grid; n is the number of users who have signed contracts with the load aggregator; P_{ui} and t_{ui} are the interrupt capacity of the i-th user and the total time of participating in the outage in the year, respectively.

LOAD FORECASTING MODEL BASED ON LSTM-SVR

Long short-term memory neural networks

LSTM belongs to a variant of recurrent neural networks. Compared with the long-term dependence problem of traditional RNN, LSTM adds gates in each cell state on the basis of RNN to control whether information is retained, which improves the problem that RNN cannot have long sequences. At present, LSTM is popularized in the processing of long sequences.

Each cell of LSTM has three parts: forgetting gate, output gate and input gate, which determine the filtering, preservation and generation of information, respectively, and the complete structure is shown in Figure 2[Wang Ke, *et al*., 2014].

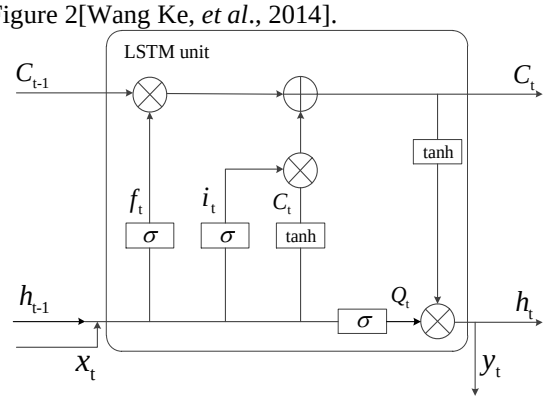

Fig.2 Structure unit of LSTM

The working steps of LSTM are as follows:

Step 1: Determine the information that needs to be filtered in the original load sequence through the forgetting gate. The current input and the previous moment input are filtered through the Sigmoid function.

$$f_t = \sigma\left[W_f\left(h_{t-1}, x_t\right) + b_f\right] \tag{23}$$

Step 2: Enter the information to decide the reserved part through the Sigmoid function. x_t and h_{t-1} are updated by the tanh function to become newly generated information cell state value $\tilde{C}_t$. The previous cell state is then updated to the current cell state value of C_t.

$$i_t = \sigma\left[W_i\left(h_{t-1}, x_t\right) + b_i\right] \tag{24}$$

$$\tilde{C}_t = \tanh\left[W_C\left(h_{t-1}, x_t\right) + b_C\right] \tag{25}$$

$$C_t = f_t C_{t-1} + i_t \tilde{C}_t \tag{26}$$

Step 3: First, the Sigmoid function determines the output part of the unit, and then the predicted value point of the model is obtained by multiplying the unit state by tanh and the gate output state.

$$o_t = \sigma\left[W_o\left(h_{t-1}, x_t\right) + b_o\right] \tag{27}$$

$$h_t = o_t \tanh C_t \tag{28}$$

Where, $\left(h_{t-1}, x_t\right)$ is the splicing vector of the current input x_t and the previous input h_{t-1}; W_f, W_i, W_C, W_o and b_f, b_i, b_C, b_o are matrix weights and bias vectors for forgetting gate f_t, input gate i_t, newly generated information cell state $\tilde{C}_t$, and output gate o_t, respectively.

Support vector regression

SVR is an efficient machine learning algorithm for solving regression problems, the essence of which is to find the optimal hyperplane to model, and minimize the "total deviation" between all sample points and the regression curve for a given prediction error set $\left(x_n, y_n\right)$. where x_n is the input load error value and y_n is the predicted load forecast. Thus, the SVR problem translates to:

$$\min_{\omega,b} \frac{1}{2}\left\|\omega^2\right\| + C\sum_{n=1}^{N} \xi_n + \hat{\xi}_n \tag{29}$$

Where, ω is the weight value; b is the bias vector; C is the penalty parameter; ξ_n and $\hat{\xi}_n$ are relaxation variables.

The corresponding constraints are:

$$\begin{cases} f\left(x_n\right) - y_n \le \varepsilon + \xi_n \\ y_n - f\left(x_n\right) \le \varepsilon + \hat{\xi}_n \\ \xi_n \ge 0, \hat{\xi}_n \ge 0, \quad n = 1, 2, \cdots, N \end{cases} \tag{30}$$

Where , ε is the regression bias.

LSTM-SVR combination model

The steps are described as follows: (1) process the raw load data, fill in the missing values and handle the outliers, and construct the three-dimensional array required for LSTM; (2) The three-dimensional array is standardized and fed into the LSTM network for training and prediction of the LSTM network, resulting in a set of predicted values; (3) The predicted result is processed with the original data to find the error term; (4) The error term is regression prediction by using the constructed SVR model, that is, the error term is corrected by SVR to obtain a new set of corrected error terms; (5) The results predicted by LSTM and the corrected error terms are combined and added to obtain the results predicted by the final

combination model. The flowchart of the LSTM-SVR algorithm is shown in Figure 3.

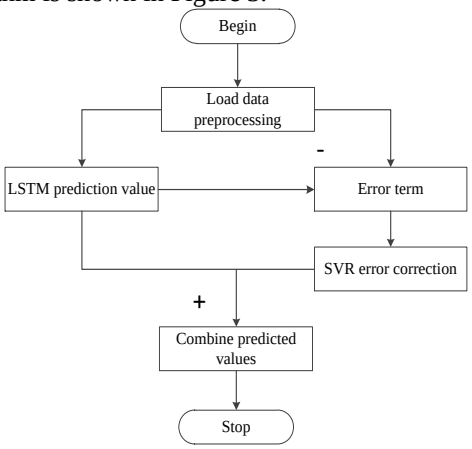

Figure 3 LSTM-SVR flowchart

Consider a load forecasting model for generalized demand-side resources

In the traditional load forecasting model, the load influencing factors include only temperature, humidity, day type, weather conditions, and historical loads. Due to the continuity and similarity of power loads, taking the load of t-th time on the d-th day as an example, the input quantity of the traditional load forecasting model in this paper is shown in Table 1.

Table 1. Input of traditional load forecasting model

Historical load	Weather and day type
$L_{t-1}^{d-1}, L_t^{d-1}, L_{t-1}^{d-2}, L_{t+1}^{d-1}, L_t^{d-2}$	$T_{\max}^d, T_{ave}^d, T_{\min}^d$
$L_{t+1}^{d-2}, L_{t-1}^{d-7}, L_t^{d-7}, L_{t+1}^{d-7}$	T_t^d, H_t^d, g^d, w^d

In Table 1, the superscript d and subscript t represent the date and time point respectively, and L_{t-1}^{d-1} is the load value of the time before the forecast day; $L_{\max}^d$, L_{ave}^d and $L_{\min}^d$ are the highest, average and lowest temperature of d-th day, T_t^d and H_t^d are the temperature and humidity of time on the d-th day, and g^d is the weather condition of d-th day. w^d is the day type of the d-th day.

In the load prediction model proposed in this paper, the main influencing factors of the output of photovoltaic and fan are light intensity and wind speed.

In order to improve the accuracy of load forecasting, the optimal scheduling scheme of electricity price, light intensity and wind speed affecting the output of photovoltaic and wind turbines, and the optimal scheduling scheme of load curtailment, load shift and interruptible load at each time of the day in the training set and test set according to the formulas (1) - (22) are used as the new input of the prediction model.

Among them, the load curtailment, load shift and interruptible load amount at the time of t-th day are $L_t^{LC,d}$, $L_t^{LS,d}$ and $L_t^{IL,d}$,and the light intensity, wind speed and real-time electricity price at time of t-th day are I_t^d, W_t^d and P_t^d, respectively, as shown in Table 2.

Table 2 Input of load forecasting model considering generalized demand-side resources

Historical load	Weather and day type	Generalized demand-side resources
$L_{t-1}^{d-1}, L_t^{d-1}, L_{t-1}^{d-2}$	$T_{\max}^d, T_{ave}^d, T_{\min}^d$	I_t^d, W_t^d, P_t^d
$L_{t+1}^{d-1}, L_t^{d-2}, L_{t+1}^{d-2}$	$T_t^d, H_t^d, g^d, \omega^d$	$L_t^{LC,d}, L_t^{LS,d}$
$L_{t-1}^{d-7}, L_t^{d-7}, L_{t+1}^{d-7}$		$L_t^{IL,d}$

In order to prove the influence of generalized demand-side resources on the accuracy of load forecasting, this paper compares the forecasting models before and after considering generalized demand-side resources by using the two influencing factors in Table 1 and Table 2 to form the input quantities of the LSTM-SVR load forecasting model.

EXAMPLE ANALYSIS

In this example, the actual load data, real-time electricity price data and weather data of the Belgian power grid from March to April 2023 were selected for simulation analysis. Weather data sources include temperature, humidity, weather conditions, light intensity, and wind speed.

Solve the generalized demand-side resource scheduling model of the contract

Since the peak period of load in this area is usually 3~6h, the maximum and minimum reduction time of load is determined by this; According to the load curve of typical days in each season, the peak load period and valley period of the region can be obtained, so as to determine the transfer period and the transferred period. The capacity of the contract should be determined based on the user-controllable capacity, but due to the lack of specific data on the user-controllable capacity in this region, the capacity value shown in Table 2 is used in this example. The daily load curve in summer has a clear load peak, so 3 LC contracts and LS contracts are designed respectively, and load reduction is carried out at the peak of the load, and part of the load is transferred to other periods; There are morning peaks and evening peaks on typical days in winter, but the difference between peaks and valleys is not large, and the two peak periods in one day can be reduced and transferred with 3 LC contracts and LS contracts, and the compensation price is lower than that of summer contracts; In spring and autumn, the fluctuation of electricity load is small, and the load level is basically similar and low, so two LC contracts and LS contracts

are designed respectively, and the compensation price is the lowest. The LC contract parameters are shown in Table 3. The parameters of each LS contract are the same as those of the LC contract, and the three parameters added to the LC contract are shown in Table 4. At the same time, assume that the maximum number of executions per day for all contracts is 1. The IL contract parameters are shown in Table 5.

Table 3 LC Contract Contents

Season	Contract	Capacity/MW	Price/($/MW)	Start-up price/$	Minimum cut-off time/h	Maximum cut time/h
Summer	1	15	40	100	3	6
	2	15	45	100	3	6
	3	15	50	100	3	6
Winter	1	15	35	100	3	6
	2	15	40	100	3	6
	3	15	45	100	3	6
Spring and autumn	1	10	25	100	3	6
	2	10	30	100	3	6

Table 4 LS Contract Contents

Season	Contract	Transfer window	The period of being transferred	Transfer rate
Summer	1	10~16	4~10	100
	2	14~20	8~14	100
	3	16~22	10~16	100
Winter	1	7~13	2~7	100
	2	13~19	19~24	100
	3	16~22	11~16	100
Spring and autumn	1	5~11	11~17	100
	2	17~23	2~8	100

Table 5 IL Contract Contents

ILContract model	The amount of interruption/ MW	Compensation price/ （MW·h）	One lasts the longest time/ h	Cumulative maximum/ h
1	10	60	2	4
2	10	80	3	5
3	18	100	3	8

For the MILP problem in the second section, this paper uses the Yalmip optimization toolbox to solve it, and if the load reduction is positive and the load increase is negative, the optimal scheduling scheme of generalized demand-side resources based on contracts under the real-time electricity price on July 1 in the region is shown in Figure 4, Figure 5 and Figure 6.

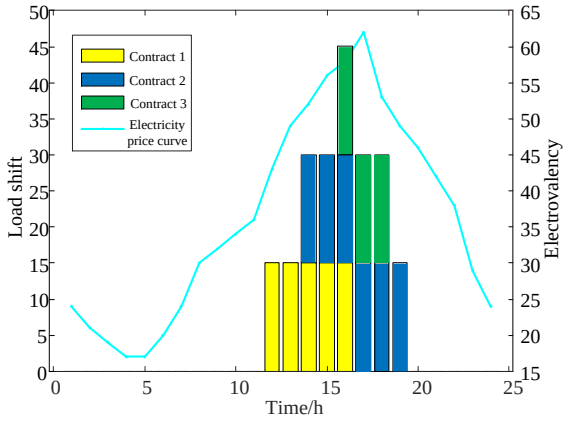

Figure 4. LS optimal scheduling scheme

The LS contract transfer capacity is shown in Figure 4. The first LS contract responds within the 12~16 period and lasts for 5h, which is due to the specified transfer period of 10~16 period, and the electricity price of period 11 is lower than the compensation electricity price; The response time of contract 2 is 14~19 periods, which does not exceed the maximum response time specified in the contract; Contract 3 only responds within the 16~18 period and lasts for 3h, although the electricity price in the 14th and 15th periods is also higher than the compensation electricity price of Contract 3, but it does not meet the specified response time, so it does not respond.

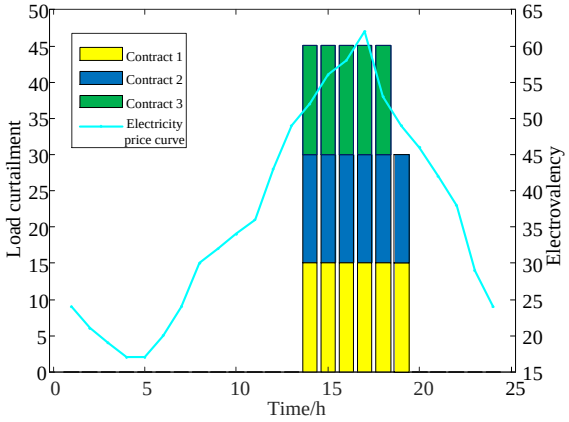

Figure 5. LC optimal scheduling scheme

The capacity reduction in the LC contract is shown in Figure 3. The first two contracts in the LC contract both dispatch can cut the load within the 14~19 period for 6h, which does not exceed the maximum response time stipulated in the contract, while contract 3 only responds in the 14~18 period and lasts for 5h, which is because the electricity price in the 19th period is lower than the compensation price of contract 3, so contract 3 only responds in the first 5h.

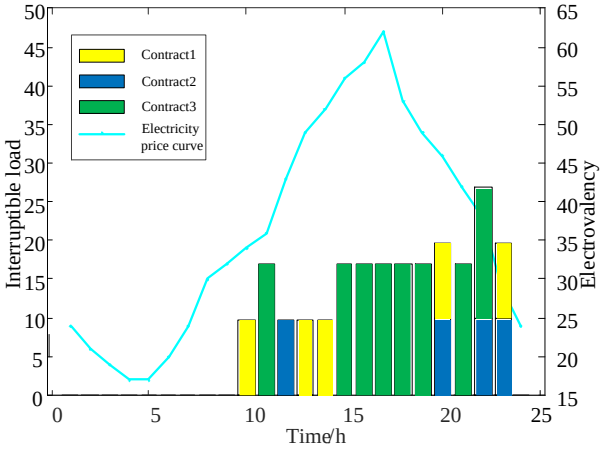

Figure 6. IL optimal scheduling scheme

The interruptible amount derived from the IL contract is shown in Figure 6. In the higher phase of the daily load curve, part of the IL resources are called. Under the condition of load IL time response characteristics, IL resources with lower purchase price are called first in the period of tight power supply, replacing the role of some high-priced peak-shaving units.

Load forecast study

In order to verify the effectiveness of the load forecasting method proposed in this paper, the load data needs to be simulated. The load reduction and load transfer obtained in Section 4.1 are the planned amount of demand response, while the actual response amount has internal instability, and the response strength is affected by changes in external factors (such as time point, meteorological conditions, electricity prices, etc.). The actual response load of the user at a certain moment is the actual impact of the planned response load at this moment, superimposed on the planned response load at other moments, and the impact amount distributed to the current moment after the planned response load is affected, and the magnitude of each external influencing factor at different times and the impact mechanism of the load are changed. Therefore, this paper constructs a linear time-varying model as follows:

$$\begin{aligned} DRL_{true}(t) &= a_0(\omega(t))DRL(t)+ \\ &a_1(\omega(t-1))DRL(t-1)+\cdots+ \\ &a_p(\omega(t-p))DRL(t-p)+\cdots+ \\ &a_{n-1}(\omega(t-n+1))DRL(t-n+1)+r(t), \end{aligned} \tag{26}$$

Among them, $r(t)$ is the zero mean independent and distributed random error partial load, $a_p(\omega(t-p))DRL(t-p)$ is the influence of the planned response load on the actual response load at time $t-p$, $a_p(\omega(t-p))$ is the percentage of the part load to the planned response load at time $t-p$,

$p=0,1,\cdots,n-1,n$ is the number of consecutive moments that affect the actual response load at time t, and the calculation formula of $a_p\left(\omega\left(t-p\right)\right)$ is as follows:

$$a_p\left(\omega\left(t-p\right)\right)=a_{p,0}+a_{p,1}\partial_1\left(\omega\left(t-p\right)\right)+ a_{p,2}\partial_2\left(\omega\left(t-p\right)\right)+a_{p,q}\partial_q\left(\omega\left(t-p\right)\right)+\cdots +a_{p,m}\partial_m\left(\omega\left(t-p\right)\right), \quad (27)$$

Among them, $\omega\left(t-p\right)$ is the vector of external influencing factors that affect the user's response at time $t-p$, $\partial_q\left(\omega\left(t-p\right)\right)$ represents the actual response load of each external influencing factor at the q-th mechanism at time $t-p$, $a_{p,q}$ is the weight of the q-th influencing mechanism at time t, and $q=0,1,\cdots,m$, m is the number of influencing mechanisms of each external influencing factor on the response load.

In this paper, model parameters are selected $n=3$, $m=1$, $a_{0,0}=0.6$, $a_{0,1}=0.01$, $a_{1,0}=0.2$, $a_{1,1}=0.01$, $a_{2,0}=0.05$, $a_{2,1}=0.01$, The influence mechanism of external factors $\partial_q\left(\omega\left(t-p\right)\right)$ is as follows:

$$\partial_1\left(\omega\left(t\right)\right)=\begin{cases}0.5t, & t\in\left[0,11\right]\\ 0.5\left(t-12\right), & t\in\left[12,23\right]\end{cases} \quad (28)$$

The actual load data for July and August in the region is used as the original actual total electricity load without generalized demand-side resources, and on this basis, the optimal scheduling planning amount of two generalized demand-side resources, cut-load and transferable load, is superimposed as the comprehensive load to be predicted. The figure shows the original load of one week and the simulated comprehensive load curve, and it can be seen that the peak-to-valley difference of the comprehensive load curve is small after the demand response, as shown in Figure 7.

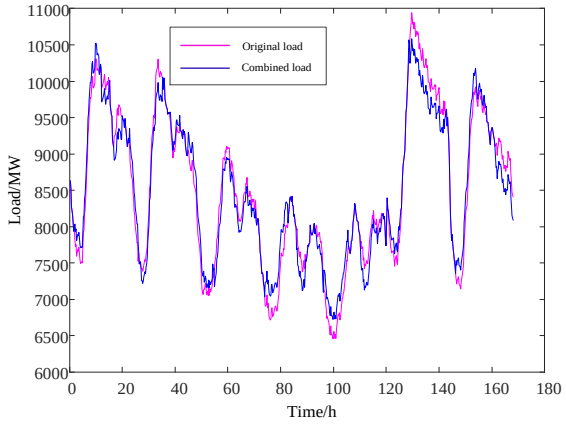

Figure 7. The curves of load before and after simulation

Model parameter setting and SVR error correction

The normalized data is divided into training and test sets to construct the LSTM load forecasting model. The number of hidden layers of LSTM affects the prediction accuracy of the model. When the number of hidden layers is large, the better the prediction effect; When the number of layers is small, the training time is correspondingly shorter. Experiments have proved that when the number of hidden layers is set to 3, it can ensure that the training time is less and the accuracy is better. The network training algorithm selects the ADMA algorithm, the number of training rounds is 150 times, the initial learning rate is set to 0.005, and the learning rate is reduced by multiplying by the attenuation factor of 0.2 after 100 training sessions. The output layer uses a fully connected layer, and the output values are reversely normalized to obtain prediction results, as shown in Figure 8.

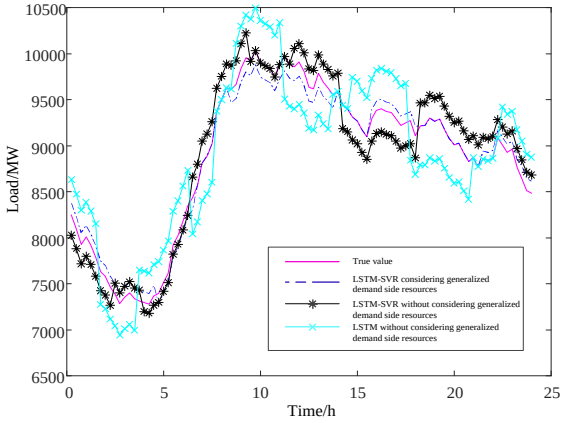

Figure 8. Comparison of prediction effects of different models

Error correction often requires the establishment of slave predictors to predict error sequences. The predicted residual series is superimposed with the initial prediction result to obtain the corrected prediction result. It indicates that the error correction model of SVR can improve the overall load prediction accuracy.

Combined with Table 5 and Figure 7, it can be seen that a single LSTM model will cause gradient vanishing due to its long sequence length, and the prediction results are obviously insufficient compared with LSTM-SVR. RMSE values, MAPE values and MAE values decreased by 8.02%, 9.71% and 12.03%, respectively, and the data fitting degree R^2 increased to 97.12%, which proved that LSTM-SVR with error correction can effectively improve the accuracy of short-term load forecasting. After considering the generalized demand-side resources, the RMSE value, MAPE value and MAE value decreased by 24.18%, 48.09% and 38.35%, respectively, and the data fitting degree R^2 increased to 98.97%, which proved that the LSTM-SVR load forecasting method considering generalized demand-side resources proposed in this paper has a good prediction effect.

Table 6 Predictive evaluation indicators of different models

Model	RMSE/MW	MAPE/%	MAE/MW	R^2
LSTM	49.8167	1.2568	35.8471	0.9653
LSTM-SVR without considering generalized demand side resources	45.8214	1.1348	31.5356	0.9712
LSTM-SVR considering generalized demand side resources	34.7365	0.5891	19.4435	0.9897

CONCLUSION

In this paper, a short-term load forecasting method of LSTM-SVR considering generalized demand-side resources is proposed. This method introduces generalized demand-side resources into market transactions through load aggregators, constructs a contract-based generalized demand-side resource scheduling model, and obtains the optimal scheduling scheme. Then, taking the optimal scheduling plan as the input quantity of the load forecasting model, an LSTM-SVR short-term load forecasting model considering generalized demand-side resources is constructed, and compared with the LSTM-based forecasting model and the LSTM-SVR forecasting model without considering generalized demand-side resources. The example verification shows that the load forecasting method considering the demand-side resources can effectively improve the accuracy of the forecast model. The proposed method is innovative, providing new methods and ideas for load forecasting. However, there are still the following shortcomings in this work: since this paper aims to predict the total amount of electricity load, the system topology and load distribution are not considered for the time being; Generalized demand-side resources include controllable load, distributed power and energy storage, etc., and this paper mainly considers the load curtailment, load shift and interruptible load in the controllable load, and not considers the influence of other factors.

REFERENCES

Bedi J, Toshniwal D. Deep learning framework to forecast electricity demand[J]. Applied energy, 2019, 238: 1312-1326.

Bergsteinsson H G, Møller J K, Nystrup P, et al. Heat load forecasting using adaptive temporal hierarchies. Applied Energy, 2021, 292: 116872.

Bian H, Zhong Y, Sun J, et al. Study on power consumption load forecast based on K-means clustering and FCM–BP model. Energy Reports, 2020, 6: 693-700.

Chen Y, Zhang D. Theory-guided deep-learning for electrical load forecasting (TgDLF) via ensemble long short-term memory. Advances in Applied Energy, 2021, 1: 100004.

Cheng Haozhong , Hu Xiao, Wang Li, et al. Review on research of regional integrated energy system planning. Automation of Electric Power Systems, 2019, 43(7): 2-13.

Ding Y, Huang C, Liu K, et al. Short-term forecasting of building cooling load based on data integrity judgment and feature transfer. Energy and Buildings, 2023, 283: 112826.

Hu M, Stephen B, Browell J, et al. Impacts of building load dispersion level on its load forecasting accuracy: Data or algorithms? Importance of reliability and interpretability in machine learning. Energy and Buildings, 2023, 285: 112896.

Jia Hong jie, Wang Dan, Xu Xiaodong, et al. Research on some key problems related to integrated energy systems. Automation of Electric power system, 2015, 4(7): 198-207.

Kang Chongqing, Yao Liangzhong. Key scientific issues and theoretical research framework for power systems with high proportion of renewable energy[J]. Automation of Electric Power System, 2017, 41(9): 1-11.

Li C, Li G, Wang K, et al. A multi-energy load forecasting method based on parallel architecture CNN-GRU and transfer learning for data deficient integrated energy systems. Energy, 2022, 259: 124967.

Li Yaping, Zhou Jing, Ju Ping, et al. Quantitative assessment method for interactive impact of flexible load[J]. Automation of Electric Power Systems, 2015, 39(17): 26-32.

Liu H, Tang Y, Pu Y, et al. Short-term load forecasting of multi-energy in integrated energy system based on multivariate phase space reconstruction and support vector regression mode[J]. Electric Power Systems Research, 2022, 210: 108066.

Nada Mounir, Hamid Ouadi, Ismael Jrhilifa. Short-term electric load forecasting using an EMD-BT-LSTM approach for smart grid energy management system. Energy and Buildings, 2023, 288: 113022.

Niu D, Yu M, Sun L, et al. Short-term multi-energy load forecasting for integrated energy systems based on CNN-BiGRU optimized by attention mechanism. Applied Energy, 2022, 313: 118801.

Qiao M, He X, Cheng X, et al. KSTAGE: A knowledge-guided spatial-temporal attention graph learning network for crop yield prediction. Information Sciences, 2023, 619: 19-37.

Rastegar M, Fotuhi M, Lehtonen M. Home load management in a residential energy hub[J]. Electric Power System Research, 2015, 119: 322-328.

Tan Z, De G, Li M, et al. Combined electricity-heat-cooling-gas load forecasting model for integrated energy system based on multi-task learning and least square support vector machine. Journal of cleaner production, 2020, 248: 119252.

Wang Ke, Yao Jianguo, Yao Liangzhong, et al. Overview of research on flexible load scheduling of electric power. Power System Automation, 2014, 38(20): 127-135.

Wang N, Zhang D, Chang H, et al. Deep learning of subsurface flow via theory-guided neural network. Journal of Hydrology, 2020, 584: 124700.

Wu Jianzhong. Drivers and state-of the-art of integrated energy systems in Europe[J]. Automation of Electric Power Systems, 2016, 40(5): 1-7.

Yang Haizhu, Li Menglong, Jiang Zhaoyang, et al. A hybrid robust system considering outliers for electric load series forecasting. Applied Intelligence, 2022: 1-23.

Zhu J, Dong H, Zheng W, et al. Review and prospect of data-driven techniques for load forecasting in integrated energy systems. Applied Energy, 2022, 321: 119269.